J Nanostruct 11(3): 534-542, Summer 2021

RESEARCH PAPER

Graphene Oxide as a Nanocarrier for Controlled Delivery of Indole

*Yasin Sadeghipour [1], Salar Hafez Ghoran [1,2] *, Mostafa Shafiee [1], Seyed AmirHossein Mousavi [1], Fatemeh Sadat Dehghani [1], Ali Mohammad Amani [1]**

[1] *Department of Medical Nanotechnology, School of Advanced Medical Sciences and Technologies, Shiraz University of Medical Sciences, Shiraz, Iran*

[2] *Department of Chemistry, Faculty of Science, Golestan University, Gorgan, Iran*

ARTICLE INFO

Article History:
Received 04 April 2021
Accepted 25 June 2021
Published 01 July 2021

Keywords:
Bioavailability
Drug delivery
Graphene oxide
Nanocarrier
pH sensitive

ABSTRACT

Regarding the specific physiochemical and biomedical properties of graphene oxide (GO), it has been a long time that experts have preferred anticancer drug cocktails to single drugs. Given that the former may develop a more balanced molecular basis for recent chemotherapeutic strategies. In this study, graphene oxide was investigated as a bioavailable nanocarrier for indoles. The synthesized components were characterized using Fourier transform infrared (FTIR), X-ray diffraction (XRD), UV–Vis spectroscopies, and scanning electron microscopy (FE-SEM) techniques. Interestingly, maximum drug loading efficiency was achieved in the neutral media (pH=7). The release analysis in different media revealed higher rate in both acidic and basic media than in neutral media. However, the total loaded drug was released in less than 80 minutes in all the systems prepared. The MTT assay results toward mesenchymal stem cells exhibited a desirable biocompatibility of GO-indole and GO. Taken together, the prepared GO-indole has suitable drug loading efficiency.

How to cite this article
Sadeghipour Y, Ghoran S. H, Shafiee M, Mousavi S. A, Dehghani F. S, Amani1 A. M. Graphene Oxide as a Nanocarrier for Controlled Delivery of Indole. J Nanostruct, 2021; 11(3):534-542. DOI: 10.22052/JNS.2021.03.011

INTRODUCTION

Studies on the nanomaterial-based drug delivery constitute a broad area of research in many fields; this is particularly true about biomedical sciences because of its valuable properties, such as high loadings, target specificity, and controlled or sustained release kinetics in suitable cases [1, 2]. Nanoparticles have shown the ability to increase drug absorption through some mechanisms, including endocytosis and exocytosis [3, 4]. A large number of nanocarriers are currently used to deliver numerous therapeutic molecules; among these nanocarriers, graphene has the potential for drug delivery [5].

Graphene is of a single-atom thickness, comprising two-dimensional planar sheets. Having discovered by Novoselov et al. in 2004 [6], the distinguished planar aromatic structure of graphene is one of the main reasons underlying its profuse ability to efficiently capture and accommodate a large number of materials, including metals, biomolecules, and fluorescent probes [7-10]. Considering the graphene's great ability to easily traverse cell membranes and deliver proteins, nucleic acids, and peptides into cells, GO can improve the cellular uptake of small drug molecules including anticancer [11], antibacterial

* *Corresponding Author Email: S_Hafezghoran@yahoo.com*
Aliamani@sums.ac.ir

[12], antiviral [13], and macromolecules [14]. The accessibility of both surfaces of GO allows significant high drug loading capacity of GO [15]. Physicochemical properties of GO have recently attracted the attention of researchers performing studies in biological sciences. Despite the fact that the oral administration of medicines is the most preferred way of medication intake, many aromatic compounds are not much soluble in water and biological gastrointestinal fluids. These properties have unfortunately reduced the rate of absorption when medicines are administered orally, and this has led to the limited use of these drugs in the treatment of diseases [16]. Furthermore, GO contains hydrophilic groups along its edges and a hydrophobic basal plane. With its polar groups, however, GO may change hydrophilic molecules into hydrophobic molecules, as in anticancer drugs, which have been widely reported to be loaded onto graphene [17]. GO has been recently examined in nano-synthesis, as a carrier of quercetin, a flavonoid active compound with its own nutritional and therapeutic properties, aromatic structure, and low aqueous solubility [18]. The superlative properties of the oxidized form of graphene, such as the small size, large specific surface area (availability of both sides of the sheet), high reactivity, easy preparation, and superior biocompatibility have proven the potential of GO for medical and biological applications. Due to the above-mentioned unique properties, functionalized types of GO have been regarded as potential carriers in biomedical sciences. Broad research has been conducted to develop drug delivery systems, especially for anticancer therapy [19]. Indole (C_8H_7N) is the major nucleus of a large group of heteroxyl compounds with numerous pharmaceutical uses. It is a colorless crystalline solid melting at 52-54°C and decomposing at 254°C [20]. It is used in substantial pharmaceutical compounds, including sumatriptan and ondansetron, which are used to treat migraine and chemotherapy-induced vomiting, respectively [21]. Moreover, indole derivatives are capable of inhibiting the proliferation of different cancer cells, such as prostate, colon, and endothelial cancer cells. above all, some researchers have pointed out various biological activities of indole compounds, including antiviral, anti-inflammatory, and anti-cancer activities [22].

The main objective of the present study was loading indole onto GO nanoparticle synthesized from graphite. Consequently, its application in drug delivery and release was also investigated under different conditions. The physicochemical structure of the nanoparticles is investigated using various techniques, including X-ray diffraction (XRD), Fourier transform infrared (FT-IR) spectroscopy, and scanning electron microscopy (SEM) (Fig. 1).

MATERIALS AND METHODS

Synthesis of Graphene Oxide

Graphene oxide was synthesized based on the modified Hammer's method [23]. Accordingly, 5 g sodium nitrate was added to the mixture of 5 g graphite powder with 50 mL H_2SO_4 (98%) and then the mixture was completely stirred at room temperature (pH= 1). The increased heat of reaction was cooled down at room temperature using ice for 2 h. Thereafter, 15 g $KMnO_4$ were slowly added to the cooled solution. It was then heated to 35°C and stirred for 2 h. 100 mL deionized water was poured into the mixture and heated again to 90°C for 30 min. By adding 30 mL H_2O_2 (30%) as the oxidant agent, the orange resultant suspension was obtained. It was then centrifuged and washed subsequently with 200 mL HCl (30%) and 200 mL deionized water. The

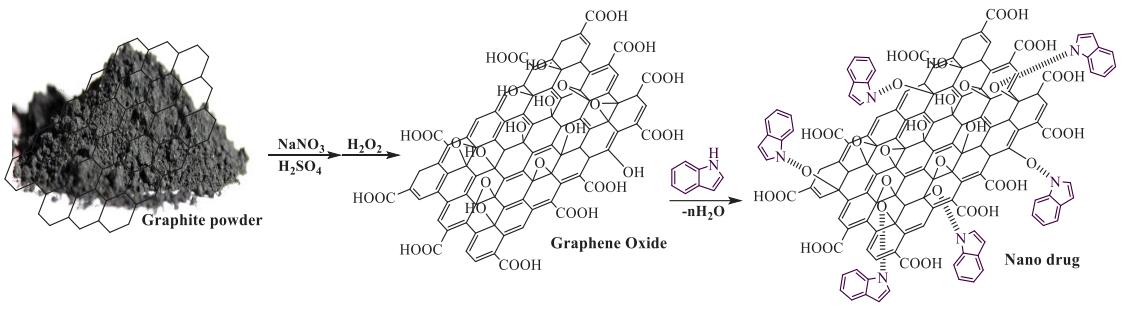

Fig. 1. Loading indole onto the graphene oxide as a nanocarrier via a chemical reaction and π-π stacking interactions.

brown yield was dried in an oven at 40°C for 24 h, which was turned into the black affirming the synthesis of graphene oxide.

Loading and release amount of indole from nanocomposite

The percentage of indole loaded onto the grapheme oxide nanocomposite was determined using a DR5000 ultraviolet-visible spectrophotometer (Hach, USA). Briefly, 0.01 g of GO was added to 10 mL of distilled water and stirred alternately for 40 minutes, using an ultrasonic stirrer. Also, 0.1 g of indole was added to 10 mL of distilled water and stirred until they were completely dissolved. The two solutions were then mixed and stirred at room temperature for 24 h. The media was centrifuged at 5000 rpm for 10 minutes. The amount of indole in the solution was estimated at a maximum wavelength (λ_{max}) of 286 nm using a standard carve of a series of standard solutions of known indole concentration. The effect of pH of the release medium was regarded as an effective factor for the release rate of Indole drug from nanocomposite. Accordingly, the pH of 500 mL of 0.1 M phosphoric acid solution was adjusted through adding 0.1 M sodium hydroxide. To measure the release rate of the drug, 0.05 g of nanoparticles was placed into 20 mL of phosphate buffer solution. The media was stirred gently, and an ultraviolet spectrophotometer was used to measure the amount of drug released into the buffer solution at the wavelength of 286 nm.

Physicochemical characterization

The FT-IR spectra were recorded at 400-4000 cm^{-1} on a FT-IR spectrometer (Perkin Elmer, Germany) using a KBr disc method. A field emission scanning electron microscope; FE-SEM (MIRA III, Czech Republic) was used to study the morphology of the synthesized nanoparticle. Spectroscopy of a single-layered GO and the synthesized nanoparticles was performed for the XRD analysis and study of the crystalline properties of the sample. The XRD technique was used to examine properties of the sample. The X-ray diffractometer (D8-ADVANCE, Germany) was used to determine the general crystal structure quantity.

In vitro cytotoxic study (MTT assay)

The toxicity and compatibility of the system were evaluated by 3-(4,5-dimethylthiazol-2-yl)-2,5-diphenyltetrazolium bromide (MTT) reduction assay [24, 25]. In summary, human mesenchymal

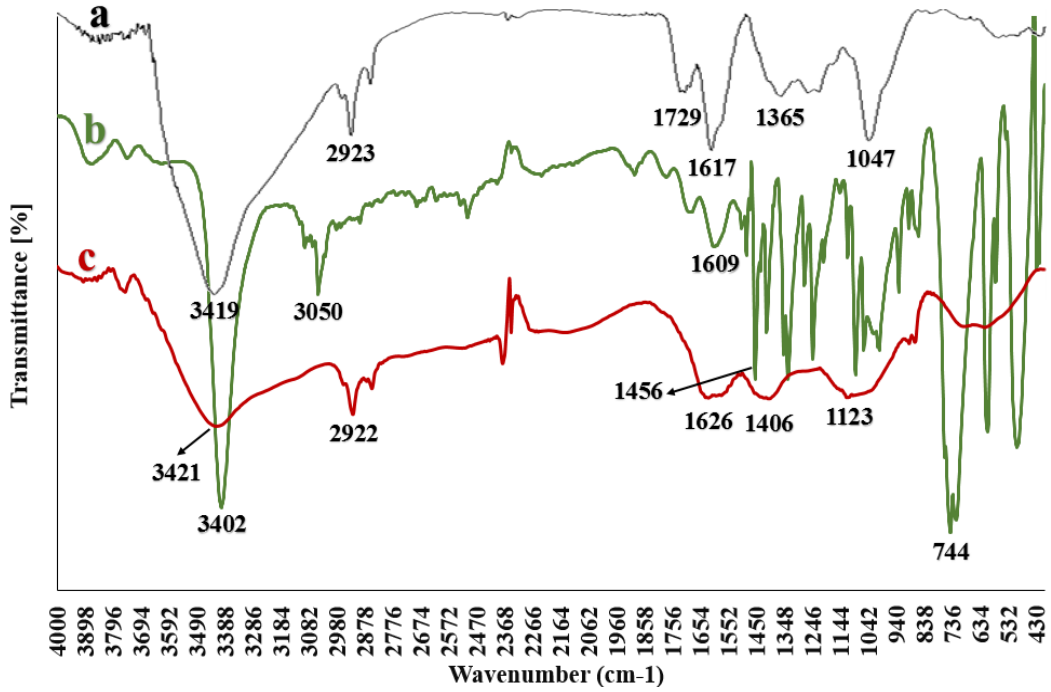

Fig. 2. The FTIR spectra of a) Graphene oxide, b) indole, and c) GO-indole nanoparticles.

stem cells (hMSCs) were cultured in a 96-well plate of a density of 20,000 cells/cm^2. After 24 h, the extracellular culture medium and 200 µL of the test medium were added to the wells. The samples were then incubated at 37°C and 5% carbon dioxide for 72 h. After the incubation period, the media (80 µL) was replaced by with 80 µL of MTT solution diluted in RPMI without phenol. After 4 h of incubation and formation of formazan crystals, the media was removed and 200 µL DMSO was added to the each well. Having used ELISA reader, the absorbance was read at the wavelength of 570 nm and compared with the absorbance of the control solution. The following equation was used to calculate the percentage of cell viability:

RESULTS AND DISCUSSION

Fourier transform infrared (FTIR) spectroscopy

The FT-IR spectra of the GO, indole, and the prepared nanoparticles were respectively analyzed in order to evaluate the chemical structures (Fig. 2). As shown in Fig. 2a previously reported [26], the band at 1047 cm^{-1} is associated with stretching vibrations of C-O bonds is in the form of carboxyl functional groups (-COOH) as well as the alcohol groups (C-OH) or the epoxy group attached to the six-membered rings with double bonds in the GO structure. The bands at the ranges of 1618-1729 cm^{-1} and 2863-2923 cm^{-1} are related to the vibrations of C=O and C-H in the form of methylene (-CH_2), respectively [27]. The band at 3419 cm^{-1} is associated with the stretching vibrations of OH groups simply attached to the rings inside GO structure [23, 28, 29]. On the other hand, the bands at 744, 1456, and 1609 cm^{-1} represent the vibrations of C-H (out-of-plane), C-C bond in the aromatic ring, and the N-H and C-C bonds in the indole structure, respectively (Fig. 2b). The broadening changes at 1123, 1406, and 1626 cm^{-1} are associated with the complete synthesis of GO-indole. The drug loading is thus confirmed considering the presence of the absorption bands of both indole and GO in the GO-indole sample (Fig. 2c).

Powder X-ray diffraction (XRD) analysis

The XRD patterns of GO, indole, and GO-indole are shown in Fig. S2 [supplementary]. Fig. S2a clearly shows the characteristic peak at 2θ=12° in the GO sample. The appearance of the characteristic peak and elimination or reduction of the graphite characteristic peak at 26° has been regarded as the sign of graphite oxidation into GO [28, 30]. Having inserted the above values in Bragg's equation, the interlayer spacing was obtained as 0.85 nm. Moreover, by comparing the individual 2θ values for GO and indole, all the spectral values were present in the synthesized GO-indole (Fig. S2c), indicating the successful loading indole onto GO. The reduced intensity of peaks might arise from the semi-crystallization of the synthetic GO-indole. By the way, the XRD results proved that the crystalline structure of the GO-indole was not distorted by the composition of GO in the GO-indole bio-nanocomposite.

Morphological analysis

Fig. 3 shows the SEM images along with the FE-SEM image of the synthesized GO-indole. Figs .3a and 3b revealed that the addition of indole on GO surface increase its roughness. It might be attributed to the relatively uniform loading and distribution of the indole onto GO, which led to condensation of structure and filling of pores. Small points show the aggregation of indole, and big planes represent the GO. There are pores smaller than 5 nm on the GO surface. Regarding the phase difference, the nano-size round masses aggregated on the GO surface were probably the GO-indole. The mean size of the aggregated particles was 61 nm.

Efficiency and quantity of indole loading

As shown in Fig. S4, the optimal conditions for reaching maximum drug loading occurred at pH 7. Almost the entire drug in the media was absorbed at the above pH and drug concentration up to 0.08 M. Therefore, the amount of the drug loaded onto GO was 4 g at the maximum drug loading of 87.08% that was reached at pH 7 (Table 1). While, a similar study has reported the maximum amount of 2.35 g of doxorubicin loaded onto GO [31].

Release kinetic of indole from graphene oxide nanocomposite

Regarding the results about release, it appears that the GO nanocarrier system alone cannot be used as an extended-release system for the drug release. The nanocarrier surface hybridization, coverage of nanocarrier surface with various polymers, and nanocarrier encapsulation can be evaluated to delay the drug release. The profile of the drug release from the drug nanocarrier

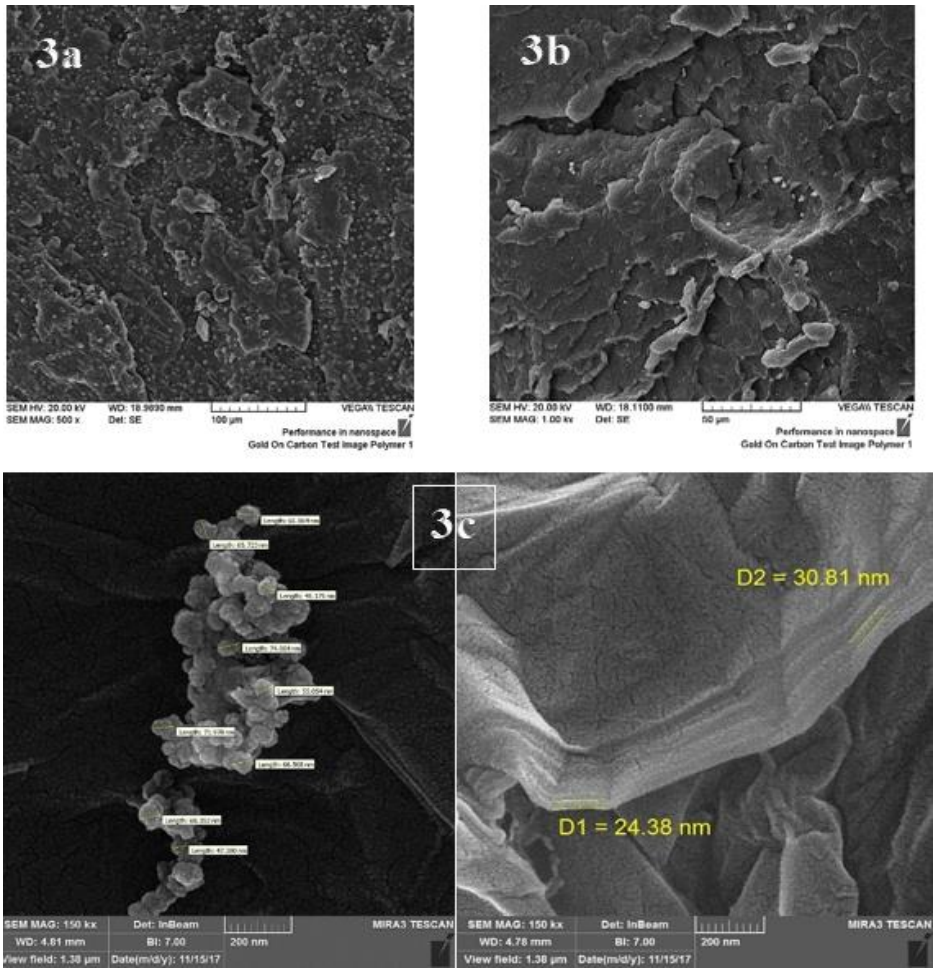

Fig. 3. The SEM images of a) GO, b) GO-indole, and c) FE-SEM image of GO-indole.

was assessed using pseudo-first order (Eq. 1) [28], pseudo-second order (Eq. 2) [32], and Korsmeyer-Peppas models (Eq. 3) [33].

$$\ln\left(\frac{q_e - q_t}{q_e}\right) = -kt \quad (1)$$

$$\frac{t}{q_t} = \frac{1}{kq_e^2} + \frac{t}{q_e} \quad (2)$$

$$\frac{M_t}{M_\infty} = kt^n \quad (3)$$

Where, q_t and q_e are the amount of released drug at t and equilibrium time (mg/g), respectively; k is the constant drug release; M_t and M_∞ are the amount of released drug at t and unlimited time (mg/g).

As shown in Fig. 4, the drug release rate was well adapted with the pseudo-second order model. The constant "n" was obtained as 0.277 from Korsmeyer-Peppas equation. It represents Fick's diffusion in the process of drug release from the system. Farazi et al, showed that the release of doxorubicin from GO-magnetite nanocomposites with the correlation coefficient of 0.99 and constant "n" of 0.45 complied with Korsmeyer-Peppas model, and the release was of a Fick's diffusion type [31].

Fig. 5 shows the effect of the pH of the release media on the release profile of the indole drug loaded in GO nanocarriers. The amount of drug released in the medium was measured regarding the amount of adsorption at the wavelength of 286 nm. As shown in Table 2, the time for release of the total loaded drug in the system in the media with pH of 3, 5, 7, 9, and 11 was respectively 20,

Table 1. The efficiency of loading the indole onto graphene oxide at different pHs and drug concentration of 0.1 M.

pH	Percentage of adsorbed drug (Drug loading efficiency) (%)	Percentage of unabsorbed drug (%)
3	47.92	52.08
5	58.33	41.67
7	87.08	12.92
9	68.65	31.35
11	21.85	85.42

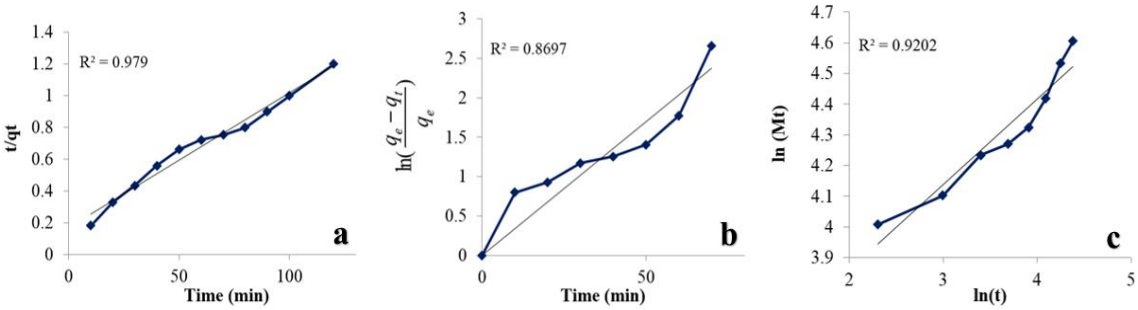

Fig. 4. Fitting the data of the indole released from GO nanocarriers in the media with pH 7.4: a) pseudo-third order, b) pseudo-first order, and c) Korsmeyer-Peppas.

Table 2. Release of indole from graphene oxide in different media in terms of time.

Time (m)	Percentage of drug released at pH 3	Percentage of drug released at pH 5	Percentage of drug released at pH 7	Percentage of drug released at pH 9	Percentage of drug released at pH 11
0	0	0	0	0	0
10	60	60	55	60	50
20	100	73	60.5	70	60
30	100	90.5	69	80	63.5
40	100	100	71.5	90	67.5
50	100	100	75.5	100	100
60	100	100	83	100	100
70	100	100	93	100	100
80	100	100	100	100	100
90	100	100	100	100	100
100	100	100	100	100	100
110	100	100	100	100	100
120	100	100	100	100	100

40, 80, 50, and 50 minutes. In this respect, the minimum drug release rate occurred at pH 7. The drug release rate in an acidic medium with pH 3 was very high to the extent that the entire loaded drug was released within 20 minutes. It could be therefore argued that the entire loaded drug was explosively released in a very short time. Moreover, the drug release rate was well adapted with the pseudo-second order model [32]. Barhouei et al. (2017) studied kinetics of the release of chlorogenic acid from GO nanocarriers using various models and reported that kinetics of the release of that drug from the system were highly adapted with the pseudo-second order model [28].

Analysis of indole toxicity

To evaluate the level of toxicity and biocompatibility of the prepared carriers, mesenchymal cells extracted from cultured bone marrow were exposed to GO suspension and GO-indole suspension. Fig. 6 shows the results of MTT assay of the samples 48 h after incubation of cells in the vicinity of the above materials. The percentage of cell viability in the sample containing GO with the concentration of 40 mg/mL

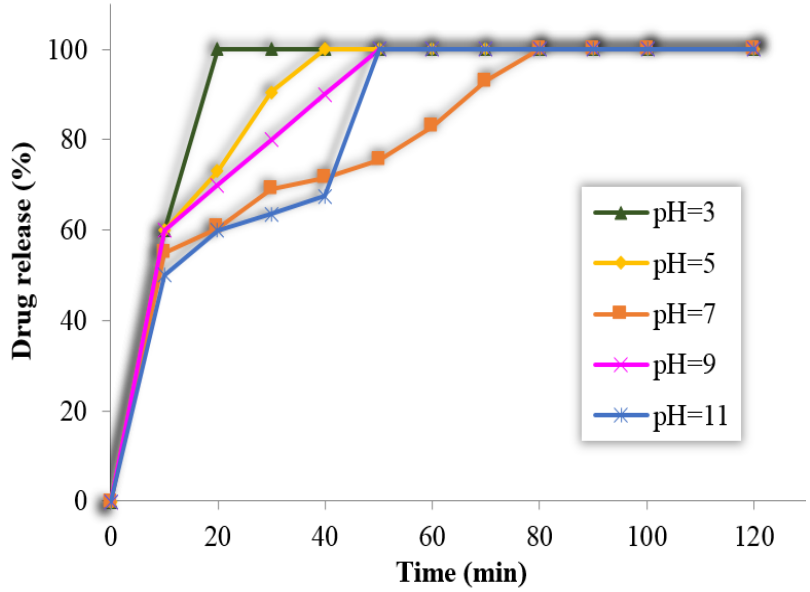

Fig. 5. The profile of the drug release from graphene oxide-indole nanocarriers at different pHs.

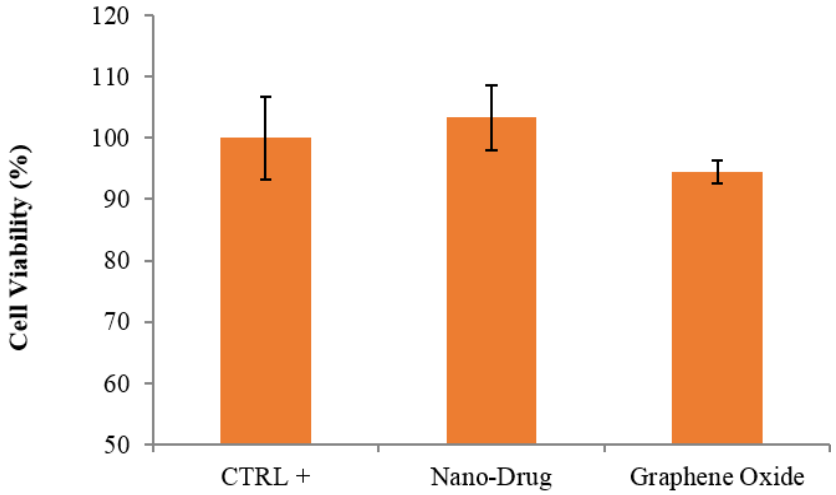

Fig. 6. Viability rate of cultured mesenchymal cells in the vicinity of suspended graphene oxide and synthesized nanoparticles at the concentration of 40 mg/ml after 72 h of incubation.

decreased to 94% ($P \leq 0.05$), and the percentage of cell viability in the GO-indole sample with the same concentration increased slightly against that in the control sample (negative control). Based on the results, the prepared drug nanocarriers did not have a toxic effect on the cultured cells and were well biocompatible.

CONCLUSIONS

To the best of our knowledge, the preparation of GO from graphite has been successfully performed using the improved Hummers' method confirmed by the FT-IR results and X-ray diffraction analyses. Indole was successfully loaded onto GO according to the FT-IR results, X-ray diffraction, and UV spectrophotometric tests. The drug loading efficiency analysis revealed that the neutral media (pH 7) was most suitable for loading indole on GO. The presence of these ions reduced the drug's affinity for the reaction with GO due to protonation and deprotonation. The evaluation of drug release in different media

revealed that the drug release rate in acidic and basic media was higher than that in the neutral medium. In all the systems designed in this study, the entire drug was released rapidly in less than 80 minutes. Acidic media contains a concentration of hydronium (H_3O^+ or H^+) that acts like a splitter or cleavage agent of the GO-indole bond and accelerates the drug release in the aqueous solution. Consequently, the loaded indole releases faster as the medium becomes acidic more and more. The GO-indole bond cleavage occurs also in less acidic or neutral media. However, more time is needed for reaching the maximum release due to the low concentration of hydronium in such media. In basic media on the other hand, hydroxide as an alternative for GO can split the GO-indole bond and takes its place. Therefore, the drug release in basic media happens faster than that in neutral media. In terms of indole release, a comparison between acidic and basic media revealed that the cleavage of the GO-indole bond occurred faster, and less time was spent for the release of the maximum loaded indole. The reason was that the hydronium played a catalytic role besides acting as a cleavage agent of the GO-indole bond. The release results showed that the total loaded drug had been released in 120 minutes. The results of stability analysis showed that the release profile of the designed system did not change after 2 months of storage under ambient conditions. The in vitro preparation of the drug nanocarriers, and GO, which were exposed to bone marrow-derived mesenchymal cells, showed appropriate biocompatibility, with over 94% of cells remained viable after 72 h of incubation of 40 mg/ml nanocarrier and GO suspension. It shall be finally noted that although the designed system showed good loading efficiency, loading rate, and biocompatibility in development of an extended-release system, the nanocarrier should undergo some structural modifications.

ACKNOWLEDGMENTS

The authors appreciate the technical support of Shiraz University of Medical Sciences, Shiraz, Iran.

CONFLICT OF INTEREST

The authors declare there is no competing interest.

REFERENCES

1. Feng T, Zhao Y. Nanomaterial-based drug delivery carriers for cancer therapy. Nanomaterial-based drug delivery carriers for cancer therapy: Springer; 2017. p. 15-54.
2. Luo L, Shu R, Wu A. Nanomaterial-based cancer immunotherapy. J. Mater. Chem. B. 2017;5(28):5517-5531.
3. Oh N, Park J-H. Endocytosis and exocytosis of nanoparticles in mammalian cells. Int. J. Nanomedicine. 2014;9:51.
4. Hafez Ghoran S, Fadaei Dashti M, Maroofi A, Shafiee M, Zare-Hoseinabadi A, Behzad F, et al. Biosynthesis of Zinc Ferrite Nanoparticles Using Polyphenol-rich extract of Citrus aurantium flowers. Nanomed. Res. J. 2020;5(1):20-28.
5. Mousavi SM, Hashemi SA, Ghasemi Y, Amani AM, Babapoor A, Arjmand O. Applications of graphene oxide in case of nanomedicines and nanocarriers for biomolecules: review study. Drug Metab. Rev. 2019;51(1):12-41. .
6. Novoselov KS, Geim AK, Morozov SV, Jiang D, Zhang Y, Dubonos SV, et al. Electric field effect in atomically thin carbon films. Science. 2004;306(5696):666-669.
7. Mousavi M, Hashemi A, Arjmand O, Amani AM, Babapoor A, Fateh MA, et al. Erythrosine adsorption from aqueous solution via decorated graphene oxide with magnetic iron oxide nano particles: kinetic and equilibrium etudies. Acta Chim. Slov. 2018;65(4):882-894.
8. Mousavi SM, Hashemi SA, Amani AM, Esmaeili H, Ghasemi Y, Babapoor A, et al. Pb (II) Removal from synthetic wastewater using kombucha scoby and graphene oxide/Fe_3O_4. Phys. Chem. Res. 2018;6(4):759-771.
9. Mousavi SM, Hashemi SA, Arjmand M, Amani AM, Sharif F, Jahandideh S. Octadecyl amine functionalized Graphene oxide towards hydrophobic chemical resistant epoxy Nanocomposites. ChemistrySelect. 2018;3(25):7200-7207.
10. Abdollahifar A, Hashemi SA, Mousavi SM, Rahsepar M, Amani AM. Fabrication of graphene oxide-lead oxide epoxy based composite with enhanced chemical resistance, hydrophobicity and thermo-mechanical properties. Adv. Polym. Technol. 2018;37(8):3792-3803.
11. Mousavi SM, Soroshnia S, Hashemi SA, Babapoor A, Ghasemi Y, Savardashtaki A, et al. Graphene nano-ribbon based high potential and efficiency for DNA, cancer therapy and drug delivery applications. Drug Metab. Rev. 2019;51(1):91-104.
12. Szunerits S, Boukherroub R. Antibacterial activity of graphene-based materials. J. Mater. Chem. B. 2016;4(43):6892-6912. doi: https://doi.org/10.1039/C6TB01647B.
13. Du T, Lu J, Liu L, Dong N, Fang L, Xiao S, et al. Antiviral activity of graphene oxide–silver nanocomposites by preventing viral entry and activation of the antiviral innate immune response. ACS Appl. Bio Mater. 2018;1(5):1286-1293.
14. Padmavathy N, Jaidev L, Bose S, Chatterjee K. Oligomer-grafted graphene in a soft nanocomposite augments mechanical properties and biological activity. Mater. Des. 2017;126:238-249.
15. Li J, Liang X, Zhang J, Yin Y, Zuo T, Wang Y, et al. Inhibiting pulmonary metastasis of breast cancer based on dual-targeting graphene oxide with high stability and drug loading capacity. Nanomedicine: NBM. 2018;14(4):1237-1248.
16. Geim AK. Graphene: status and prospects. Science. 2009;324(5934):1530-1534.
17. Javanbakht S, Namazi H. Doxorubicin loaded carboxymethyl cellulose/graphene quantum dot nanocomposite hydrogel films as a potential anticancer drug delivery system. Mater.

Sci. Eng: C. 2018;87:50-59. doi: https://doi.org/10.1016/j.msec.2018.02.010.
18. Rahmanian N, Hamishehkar H, Dolatabadi JEN, Arsalani N. Nano graphene oxide: a novel carrier for oral delivery of flavonoids. Colloids Surf. B: Biointerfaces. 2014;123:331-338.
19. Zuchowska A, Chudy M, Dybko A, Brzozka Z. Graphene as a new material in anticancer therapy-in vitro studies. Sens. Actuators B: Chem. 2017;243:152-165. .
20. Barden TC. Indoles: industrial, agricultural and over-the-counter uses. Heterocyclic Scaffolds II:: Springer; 2010. p. 31-46.
21. Stieler JM, Reichardt P, Riess H, Oettle H. Treatment options for chemotherapy-induced nausea and vomiting. Am. J. Cancer. 2003;2(1):15-26.
22. Ahmad A, A Sakr W, Wahidur Rahman K. Anticancer properties of indole compounds: mechanism of apoptosis induction and role in chemotherapy. Curr. Drug Targets. 2010;11(6):652-666.
23. Fan L, Ge H, Zou S, Xiao Y, Wen H, Li Y, et al. Sodium alginate conjugated graphene oxide as a new carrier for drug delivery system. Int. J. Biol. Macromol. 2016;93:582-590.
24. Hafez Ghoran S, Rahimi H, Kazemi A, Scognamiglio M, Naderian M, Iraji A, et al. Allium hooshidaryae (Alliaceae); Chemical compositions, biological and ethnomedicine uses. J. Ethnopharmacol. 2021;274:113918.
25. Hafez Ghoran S, Firuzi O, Asadollahi M, Stuppner H, Alilou M, Jassbi AR. Dammarane-type triterpenoid saponins from Salvia russellii Benth. Phytochemistry. 2021;184:112653..
26. Dreyer DR, Murali S, Zhu Y, Ruoff RS, Bielawski CW. Reduction of graphite oxide using alcohols. J. Mater. Chem. 2011;21(10):3443-3447.
27. Marcano DC, Kosynkin DV, Berlin JM, Sinitskii A, Sun Z, Slesarev A, et al. Improved synthesis of graphene oxide. ACS nano. 2010;4(8):4806-4814.
28. Barahuie F, Saifullah B, Dorniani D, Fakurazi S, Karthivashan G, Hussein MZ, et al. Graphene oxide as a nanocarrier for controlled release and targeted delivery of an anticancer active agent, chlorogenic acid. Mater. Sci. Eng: C. 2017;74:177-185.
29. Ma N, Liu J, He W, Li Z, Luan Y, Song Y, et al. Folic acid-grafted bovine serum albumin decorated graphene oxide: an efficient drug carrier for targeted cancer therapy. J. Colloid Interface Sci. 2017;490:598-607.
30. Zhang W, Shi X, Zhang Y, Gu W, Li B, Xian Y. Synthesis of water-soluble magnetic graphene nanocomposites for recyclable removal of heavy metal ions. J. Mater. Chem. A. 2013;1(5):1745-1753.
31. Farazi R, Vaezi MR, Molaei MJ, Saeidifar M, Behnam ghader AA. Drug loading and release behavior of graphene oxide/magnetite nanocomposite. J. Adv. Mater. Technol. 2017;6(1):33-41.
32. Ho Y-S, Ofomaja AE. Pseudo-second-order model for lead ion sorption from aqueous solutions onto palm kernel fiber. J. Hazard. Mater. 2006;129(1-3):137-142.
33. Dong L, Yan L, Hou W-G, Liu S-J. Synthesis and release behavior of composites of camptothecin and layered double hydroxide. J. Solid State Chem. 2010;183(8):1811-1816.